Warm spring reduced carbon cycle impact of the 2012 US summer drought

Sebastian Wolf[a,b,1], Trevor F. Keenan[c,2], Joshua B. Fisher[d], Dennis D. Baldocchi[a], Ankur R. Desai[e], Andrew D. Richardson[f], Russell L. Scott[g], Beverly E. Law[h], Marcy E. Litvak[i], Nathaniel A. Brunsell[j], Wouter Peters[k,l], and Ingrid T. van der Laan-Luijkx[k]

[a]Department of Environmental Science, Policy, and Management, University of California, Berkeley, CA 94720; [b]Department of Environmental Systems Science, ETH Zurich, 8092 Zurich, Switzerland; [c]Department of Biological Sciences, Macquarie University, Sydney, NSW 2109, Australia; [d]Jet Propulsion Laboratory, California Institute of Technology, Pasadena, CA 91109; [e]Atmospheric and Oceanic Sciences, University of Wisconsin–Madison, Madison, WI 53706; [f]Department of Organismic and Evolutionary Biology, Harvard University, Cambridge, MA 02138; [g]US Department of Agriculture, Agricultural Research Service, Southwest Watershed Research Center, Tucson, AZ 85719; [h]Department of Forest Ecosystems and Society, Oregon State University, Corvallis, OR 97331; [i]Department of Biology, University of New Mexico, Albuquerque, NM 87131; [j]Department of Geography, University of Kansas, Lawrence, KS 66045; [k]Department of Meteorology and Air Quality, Wageningen University, 6708 PB Wageningen, The Netherlands; and [l]Centre for Isotope Research, University of Groningen, 9747 AG Groningen, The Netherlands

Edited by Susan E. Trumbore, Max Planck Institute for Biogeochemistry, Jena, Germany, and approved March 22, 2016 (received for review October 3, 2015)

The global terrestrial carbon sink offsets one-third of the world's fossil fuel emissions, but the strength of this sink is highly sensitive to large-scale extreme events. In 2012, the contiguous United States experienced exceptionally warm temperatures and the most severe drought since the Dust Bowl era of the 1930s, resulting in substantial economic damage. It is crucial to understand the dynamics of such events because warmer temperatures and a higher prevalence of drought are projected in a changing climate. Here, we combine an extensive network of direct ecosystem flux measurements with satellite remote sensing and atmospheric inverse modeling to quantify the impact of the warmer spring and summer drought on biosphere-atmosphere carbon and water exchange in 2012. We consistently find that earlier vegetation activity increased spring carbon uptake and compensated for the reduced uptake during the summer drought, which mitigated the impact on net annual carbon uptake. The early phenological development in the Eastern Temperate Forests played a major role for the continental-scale carbon balance in 2012. The warm spring also depleted soil water resources earlier, and thus exacerbated water limitations during summer. Our results show that the detrimental effects of severe summer drought on ecosystem carbon storage can be mitigated by warming-induced increases in spring carbon uptake. However, the results also suggest that the positive carbon cycle effect of warm spring enhances water limitations and can increase summer heating through biosphere–atmosphere feedbacks.

seasonal climate anomalies | carbon uptake | ecosystem fluxes | biosphere–atmosphere feedbacks | eddy covariance

An increase in the intensity and duration of drought (1, 2), along with warmer temperatures, is projected for the 21st century (3). Warmer and drier summers can substantially reduce photosynthetic activity and net carbon uptake (4). In contrast, warmer temperatures during spring and autumn prolong the period of vegetation activity and increase net carbon uptake in temperate ecosystems (5), sometimes even during spring drought (6). Atmospheric CO_2 concentrations suggest that warm-spring–induced increases in carbon uptake could be cancelled out by the effects of warmer and drier summers (7). However, the extent and variability of potential compensation on net annual uptake using direct observations of ecosystem carbon exchange have not yet been examined for specific climate anomalies.

In addition to perturbations of the carbon cycle, warmer spring temperatures can have an impact on the water cycle by increasing evaporation from the soil and plant transpiration (8–10), which reduces soil moisture. Satellite observations suggest that warmer spring and longer nonfrozen periods enhance summer drying via hydrological shifts in soil moisture status (11). Climate model simulations also indicate a soil moisture–temperature feedback between early vegetation green-up in spring and extreme temperatures in summer (12, 13). Soil water deficits during drought impose a reduction in stomatal conductance, thereby reducing evaporative cooling and thus increasing near-surface temperatures (14). Stomatal closure also has a positive (enhancing) feedback with atmospheric water demand by increasing the vapor pressure deficit (VPD) of the atmosphere (15). The vegetation response thus plays a crucial role for temperature feedbacks during drought (16).

Given the opposing effects of concurrent warmer spring and summer drought, and an increased frequency of these anomalies projected until the end of this century (*SI Appendix*, Fig. S1), it is imperative to understand (*i*) the response of the terrestrial carbon balance and (*ii*) the interaction of carbon uptake with water and energy fluxes that are associated with these seasonal climate anomalies.

The year 2012 was among the warmest on record for the contiguous United States (CONUS), which experienced one of

Significance

Carbon uptake by terrestrial ecosystems mitigates the impact of anthropogenic fossil fuel emissions on atmospheric CO_2 concentrations, but the strength of this carbon sink is highly sensitive to large-scale extreme climate events. In 2012, the United States experienced the most severe drought since the Dust Bowl period, along with the warmest spring on record. Here, we quantify the impact of this climate anomaly on the carbon cycle. Our results show that warming-induced earlier vegetation activity increased spring carbon uptake, and thus compensated for reduced carbon uptake during the summer drought in 2012. This compensation, however, came at the cost of soil moisture depletion from increased spring evapotranspiration that likely enhanced summer heating through land-atmosphere coupling.

Author contributions: S.W., T.F.K., J.B.F., D.D.B., A.R.D., and A.D.R. designed research; S.W. performed research; S.W. analyzed data; S.W., T.F.K., J.B.F., D.D.B., A.R.D., A.D.R., R.L.S., B.E.L., M.E.L., N.A.B., W.P., and I.T.v.d.L.-L. wrote the paper; S.W. compiled the flux datasets; T.F.K. performed the flux data gap-filling and partitioning; J.B.F. compiled and processed the Moderate Resolution Imaging Spectroradiometer (MODIS) and Coupled Model Intercomparison Project Phase 5 (CMIP5) data; A.R.D. performed the CarbonTracker analysis (CT2013B); and W.P. and I.T.v.d.L.-L. performed the CarbonTracker analysis (CTE2014 and CTE2015).

The authors declare no conflict of interest.

This article is a PNAS Direct Submission.

Data deposition: The eddy-covariance data are available in the AmeriFlux data archive at the Carbon Dioxide Information Analysis Center at the Oak Ridge National Laboratory (cdiac.ornl.gov/ftp/ameriflux/data).

See Commentary on page 5768.

[1]To whom correspondence should be addressed. Email: sewolf@ethz.ch.

[2]Present address: Earth and Environmental Sciences, Lawrence Berkeley National Laboratory, Berkeley, CA 94720.

This article contains supporting information online at www.pnas.org/lookup/suppl/doi:10.1073/pnas.1519620113/-/DCSupplemental.

the most severe droughts since the Dust Bowl era of the 1930s (17, 18). The drought caused substantial economic damage, particularly for agricultural production (*SI Appendix*). Annual mean temperatures were 1.8 °C above average, with the warmest spring (+2.9 °C) and second warmest summer (+1.4 °C) in the period of 1895–2012 (19). Precipitation deficits started to evolve in May across the Great Plains and the Midwest (17), but eventually affected more than half of the United States (20). By July, 62% of the United States experienced moderate to exceptional drought, which was the largest spatial extent of drought for the United States since the Dust Bowl era (19). Severe drought conditions with depleted soil moisture persisted throughout summer, and unprecedented precipitation deficits of 47% below normal for May through August were observed in the central Great Plains (17).

Here, we analyze the response of land-atmosphere carbon and water exchange for major ecosystems in the United States during the concurrent warmer spring and summer drought of 2012 at the ecosystem, regional, and continental scales. We combine direct measurements of land-atmosphere CO_2, water vapor, and energy fluxes from 22 eddy-covariance (EC) towers across the United States (*SI Appendix*, Fig. S2 and Table S1) with large-scale satellite remote-sensing observations of gross primary production (GPP), evapotranspiration (ET), and enhanced vegetation index (EVI) derived from the space-borne Moderate Resolution Imaging Spectroradiometer (MODIS), and estimates of net ecosystem production (NEP; i.e., net carbon uptake) from an atmospheric CO_2 inversion (CarbonTracker, CTE2014). This comprehensive suite of standardized analyses across sites and data streams was crucial to constrain the impact of such a large-scale drought event with bottom-up and top-down approaches (21), and something only a few synthesis studies have achieved so far (4, 22).

We test the hypothesis that increased carbon uptake due to warm spring offset the negative impacts of severe summer drought during 2012, and examine the relationship between early-spring–induced soil water depletion and increased summer temperatures. When using the term "drought," we refer to precipitation deficits that resulted in soil moisture deficiencies (9).

Results

Evidence from in Situ Measurements. At the site scale, spring (March–May) 2012 anomalies of net carbon uptake significantly increased with temperature (Fig. 1*A*), on average by 15 ± 13 g C m^{-2} $season^{-1}$ (mean ± uncertainty: +29%, $n = 22$; *SI Appendix*, Table S2) across all sites, relative to the baseline 2008–2010. This increase was linked to earlier and increased vegetation activity (*SI Appendix*, Table S3). Some sites also experienced precipitation deficits during spring, but the effect on net carbon uptake across sites was not significant (*SI Appendix*, Fig. S3). In contrast, summer (June–August) net carbon uptake decreased at most sites by 24 ± 18 g C m^{-2} $season^{-1}$ (−17%, $n = 22$), and these reductions were highly correlated with drought intensity ($R^2 = 0.64$, $P < 0.001$; Fig. 1*B*).

Of all sites, 13 (59%) experienced summer drought conditions with precipitation deficits of at least 10% or 19–326 mm $season^{-1}$ (*SI Appendix*, Fig. S2 and Table S4). Subsequently, these sites were used to investigate the process level impact of concurrent warmer spring and summer drought at the ecosystem scale.

Spring net carbon uptake increased on average by 25 ± 11 g C m^{-2} $season^{-1}$ (+103%, $n = 13$), and summer uptake decreased by 32 ± 18 g C m^{-2} $season^{-1}$ (−25%) at sites that experienced summer drought (Fig. 2). Consequently, a warmer spring compensated, on average, for 78% of drought-related reductions in summer net carbon uptake, and reduced the impact of summer drought on annual net carbon uptake to −17 ± 18 g C m^{-2} $season^{-1}$ (−11% compared with baseline; Fig. 2). A consistent, although smaller, partial compensation pattern was detected for GPP at summer drought-affected sites from both direct EC measurements (40% compensation) and satellite-derived MODIS GPP estimates (39% compensation; *SI Appendix*, Figs. S4 and S5).

Large-Scale Carbon Cycle Impact. At the regional scale, the Great Plains ecoregion (23) experienced the strongest drought conditions during summer (*SI Appendix*, Table S5), with reductions of 123 g C m^{-2} $season^{-1}$ (−36%) in GPP from MODIS estimates (Fig. 3 and *SI Appendix*, Table S6). NEP estimates from inverse modeling by CarbonTracker (CTE2014) showed reductions of 71 g C m^{-2} $season^{-1}$ (−72%) in net carbon uptake in the Great Plains, which exceeded the reductions in other ecoregions (*SI Appendix*, Table S6). Substantial summer reductions were also found for the Northern Forests ecoregion (GPP: −114 g C m^{-2} $season^{-1}$, NEP: −38 g C m^{-2} $season^{-1}$) and for the Eastern Temperate Forests ecoregion (GPP: −86 g C m^{-2} $season^{-1}$, NEP: −17 g C m^{-2} $season^{-1}$), which includes large parts of the Midwest. During the warm spring of 2012, these three ecoregions also had among the strongest increases in GPP, ranging from 32 to 75 g C m^{-2} $season^{-1}$ (*SI Appendix*, Table S6), which was particularly evident across the Appalachians (Fig. 3*A*) because tree phenology benefitted substantially from warmer temperatures during spring (*SI Appendix*, Fig. S6). The Eastern Temperate Forests showed by far the highest increase in spring NEP (69 g C m^{-2} $season^{-1}$). Annual net carbon uptake in the Great Plains was reduced by 46 g C m^{-2} y^{-1}, making the ecoregion close to carbon neutral in 2012 (−5 g C m^{-2} y^{-1} vs. baseline: 41 ± 24 g C m^{-2} y^{-1}). In contrast, the Eastern Temperate Forests had the highest net uptake during the last decade in 2012 (136 g C m^{-2} y^{-1}) and were outside the interannual variability from 2001 to 2011 (58 ± 19 g C m^{-2} y^{-1}).

Across the entire CONUS, NEP estimates by CarbonTracker showed total increases of 0.24 Pg C $season^{-1}$ during spring and reductions of 0.23 Pg C $season^{-1}$ in summer 2012 (see *SI Appendix*, Table S6 for mean values in g C m^{-2}). In 2012, spring net carbon uptake (0.76 Pg C $season^{-1}$) was the highest and summer carbon

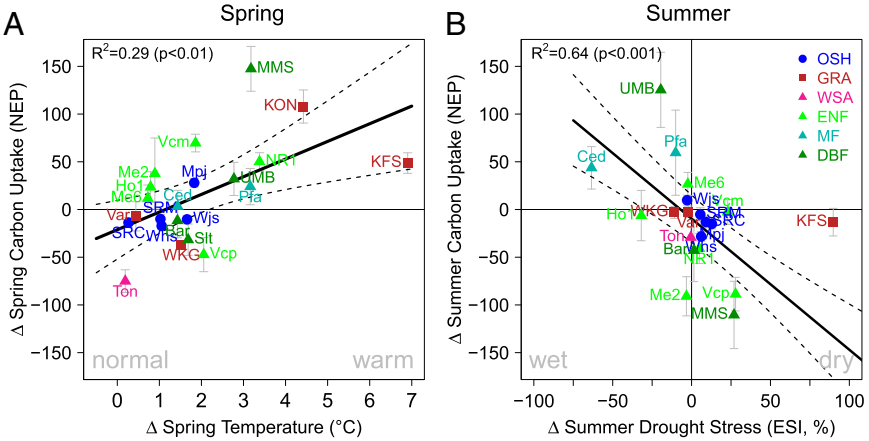

Fig. 1. Seasonal climate anomalies increased net carbon uptake in spring but led to reductions in summer throughout the United States in 2012. Flux tower-derived seasonal anomalies of NEP (g C m^{-2}) during spring (*A*) and summer (*B*; related to drought stress via the ESI) in 2012 relative to the baseline of 2008–2010. Symbols and colors denote the International Geosphere-Biosphere Program (IGBP) land-use classes, which are provided with the site names and abbreviations in *SI Appendix*, Table S1. Error bars denote the uncertainties in the flux anomalies. Dashed lines represent the confidence interval of the ordinary least squares mean regression (bold line). The summer anomaly at the site KON is out of scale (*SI Appendix*, Table S10) and was omitted from display only. Further details are provided in *SI Appendix*, Figs. S3, S15, and S16).

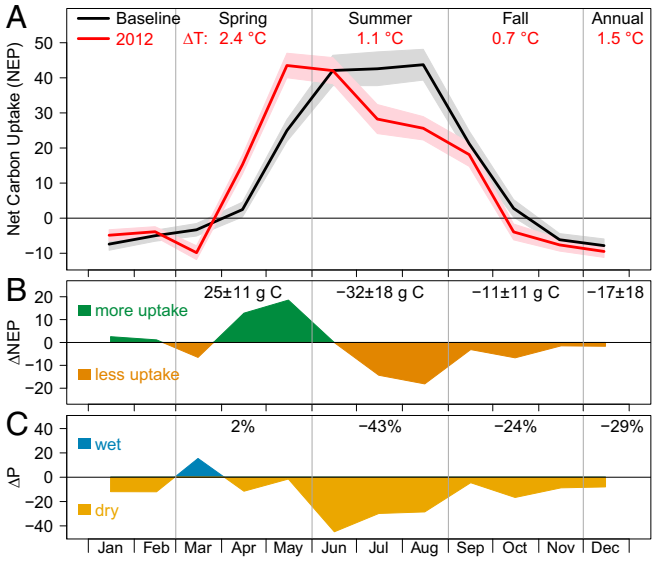

Fig. 2. Net carbon uptake of concurrent warm spring and summer drought in 2012. (*A*) Ensemble mean of EC-measured monthly NEP (g C m^{-2} mo^{-1}) for 2012 (red) and baseline (black) at sites that experienced drought during summer 2012 (n = 13). Numbers atop show the mean seasonal temperature (T) anomalies in 2012 relative to the baseline of 2008–2010. (*B*) Anomalies of NEP (g C m^{-2} mo^{-1}) in 2012 relative to the mean baseline; numbers atop denote the seasonal anomalies (g C m^{-2}) and their uncertainties, which were derived from Monte-Carlo simulations of monthly fluxes (also shading in *A*). (*C*) Anomalies of monthly precipitation (mm mo^{-1}) in 2012 relative to baseline; numbers atop show seasonal anomalies. Similar ensemble analyses for GPP and SPI can be found in *SI Appendix*, Fig. S4.

uptake was the lowest (0.38 Pg C $season^{-1}$), and both seasons were clearly outside the interannual variability across the CONUS during the last decade (*SI Appendix*, Table S7). Due to the compensation of drought-induced reductions in summer by increases from warm spring, and lower carbon losses during winter and fall (Fig. 3*H*), net annual carbon uptake across the CONUS was above average in 2012 (0.11 Pg C y^{-1}). Net annual carbon uptake in 2012 (0.33 Pg C y^{-1}) was the second highest estimated by CarbonTracker since 2001 and outside the interannual variability of the baseline (0.22 ± 0.05 Pg C y^{-1}; *SI Appendix*, Table S7).

Water and Energy Flux Feedback. Across all EC sites (n = 22), summer increases in sensible heat (H) flux were highly correlated with reductions in ET or latent energy (LE; $R^2 = 0.54$, $P < 0.001$; *SI Appendix*, Fig. S7). At sites with summer drought, we observed LE increases of 38 ± 15 MJ m^{-2} $season^{-1}$ (mean ± uncertainty: +14%, n = 13) during early spring and reductions of −66 ± 24 MJ m^{-2} $season^{-1}$ (−12%) during summer 2012 relative to baseline (*SI Appendix*, Fig. S8). This reduction in evaporative cooling was associated with soil water limitations and elevated VPD (*SI Appendix*, Table S8) causing stomatal closure. Increased ET during spring and reduced ET during summer were also evident from MODIS, both for these sites and at larger regional to continental scales (*SI Appendix*, Figs. S9 and S6). At the sites with summer drought, our results indicate that the warming-induced increase in vegetation activity during spring caused an earlier depletion of water resources (*SI Appendix*, Figs. S8 and S9), and thus contributed to soil water limitations during summer. This depletion resulted in a relative heating contribution from increased H during the period of peak insolation in summer (*SI Appendix*, Fig. S8).

To evaluate the magnitude of a potential summer heating enhancement by earlier spring vegetation activity, we quantified the impact for sites located in the center of the drought in the Midwest (Fig. 4). These sites had summer precipitation deficits of −300 ± 26 mm $season^{-1}$ (−74%, mean ± SD), and spring temperatures were warmer by 4.8 ± 1.9 °C (*SI Appendix*, Fig. S10). Earlier vegetation activity was evident in site observations of GPP (Fig. 4*C*) and satellite EVI (*SI Appendix*, Fig. S11), resulting in increased LE, and induced an earlier drawdown in soil moisture (Fig. 4*D*). Daily soil moisture was highly and negatively correlated to LE ($R^2 = 0.72$, $P < 0.001$) and GPP ($R^2 = 0.73$, $P < 0.001$) during spring 2012. At the beginning of summer, cumulative ET since January 1 was, on average, 40 mm (98 MJ m^{-2}, 26%) higher, which was a 12-d forward shift in the total amount of evaporated water compared with the baseline. During summer, evaporative cooling through LE was reduced by −201 ± 32 MJ m^{-2} $season^{-1}$ (−24%), with the majority of excess energy released through increased H (178 ± 19 MJ m^{-2} $season^{-1}$ or 107%; Fig. 4*A*). This increase in H had a relative heating effect (Fig. 4*B*) that exceeded elevated incoming shortwave radiation (*SI Appendix*, Fig. S12) and likely contributed to anomalous surface heating of 2.0 ± 1.7 °C (*SI Appendix*).

Discussion

Our results consistently show increased carbon uptake in spring and substantial reductions during summer in 2012 across independent observations at the site scale and at the regional to continental scale. This study provides further evidence from direct observations for an offset in summer reductions by a warmer spring (7). Increased vegetation activity during the warm spring in 2012 (24) compensated for reductions in net carbon uptake by the severe summer drought. Consequently, the CONUS area remained a carbon sink of 0.33 Pg C y^{-1} during 2012. In comparison, the European 2003 summer drought resulted in a carbon source of 0.50 Pg C y^{-1}, equivalent to 4 y of carbon uptake across Europe (4). A longer lasting drought in western North America reduced carbon uptake by 0.03–0.30 Pg C y^{-1} during 2000–2004 but did not turn this region into a carbon source (22). More recently, the 2011 Texas drought was reported to have reduced net carbon uptake by 0.23 Pg C y^{-1}, which was the largest anomaly in this region since 1950 (25).

Regional estimates of net carbon uptake in 2012 showed that 71% of the total summer reductions across the CONUS originated from the Great Plains (−0.16 Pg C $season^{-1}$), whereas 74% of the increased spring uptake originated from the Eastern Temperate Forests (0.18 Pg C y^{-1}). It can therefore be argued that the higher spring uptake in the Eastern Temperate Forests was the main reason that the large-scale 2012 summer drought did not result in reductions of net annual carbon uptake across the CONUS. This spring compensation emphasizes the important ecosystem service of forests for climate and their contrasting response to climate anomalies compared with grasslands (6, 16). Ensemble EC site-scale measurements showed good agreement with the continental-scale estimates by MODIS and CarbonTracker, suggesting that this ensemble of sites represents the large-scale impact of the 2012 climate anomaly across the CONUS quite well. Our results show that the carbon cycle anomaly during spring and summer 2012 was outside the range of data uncertainty (for EC sites; Fig. 2*A*) and also outside the large-scale interannual variability (for MODIS and CarbonTracker CTE2014) compared with the baseline (Fig. 3 *G* and *H*). Although EC measurements across all sites were not available before 2008, long-term observations from MODIS and CarbonTracker provide evidence that the baseline years were within the 2001–2011 seasonal variability for carbon fluxes across the CONUS, yet higher during summer (*SI Appendix*, Table S7). Long-term precipitation data show that summer was slightly wetter (+3%) during the baseline period, although with similar variability compared with the reference period (*SI Appendix*, Fig. S13 and Table S5). Consequently, by comparing the extremely dry summer of 2012 with a wetter than normal baseline period, we potentially overestimate the carbon cycle impact of the 2012 event. Using MODIS and CarbonTracker data since 2001, we estimate that the potential bias from our baseline selection for the continental-scale impact of 2012 is 11% or less seasonally and 10% or less annually (*SI Appendix*, Table S7). Given the magnitude of the 2012 drought, uncertainties due to baseline selection thus play a minor role for the large-scale impact assessment.

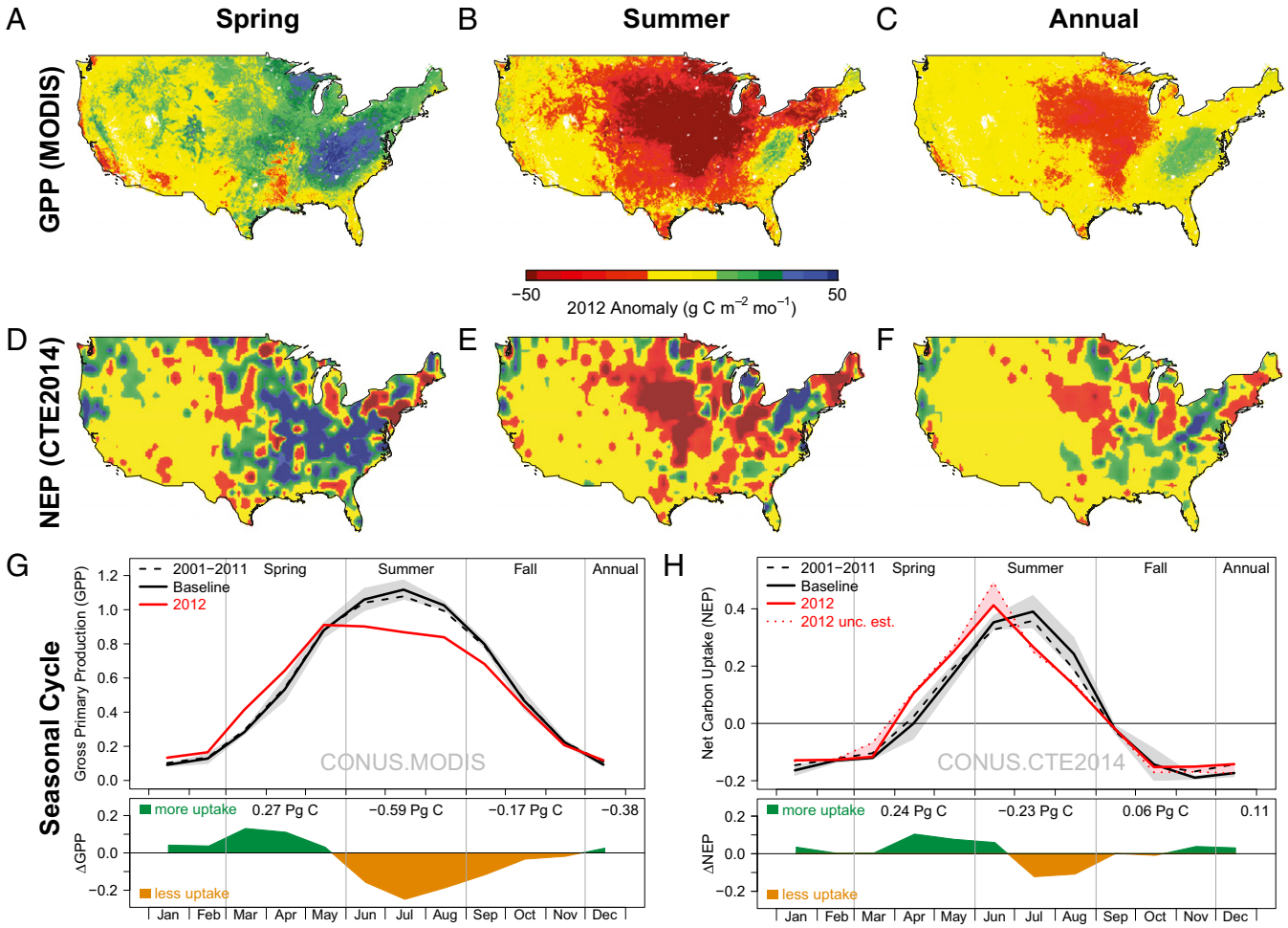

Fig. 3. Increased carbon uptake in the eastern United States during the warm spring of 2012 compensated for large reductions by the summer drought in the Midwest. Spatiotemporal anomalies are shown for GPP (g C m^{-2} mo^{-1}) from MODIS (*A*–*C*) and NEP (g C m^{-2} mo^{-1}) from CarbonTracker (CTE2014; *D*–*F*) during spring, summer, and annually in 2012 relative to the baseline of 2008–2010. Red/orange colors indicate negative anomalies (reductions), and green/blue colors show positive anomalies (increases). The seasonal cycle of total monthly GPP (*G*) and NEP (*H*) (both in Pg C) for the long-term mean (2001–2011, black dashed line), the baseline (black line), and 2012 (red line) integrated across the CONUS. The red dotted line for NEP indicates an uncertainty estimate of CTE2014, based on the independent model run CTE2015. The red shading indicates the 2012 uncertainty range between both model runs. The gray shading indicates the interannual variability (SD) during the baseline. Colored shading in lower panels shows the 2012 anomalies (Pg C) relative to the mean baseline; numbers atop denote seasonal anomalies. Further maps with spatial drought patterns (ESI, SPI), vegetation activity (EVI), and ET can be found in *SI Appendix*, Fig. S6.

Due to the coupling of ecosystem carbon and water fluxes, the warmer spring also increased ET, and thus depleted soil water resources earlier. In 2012, soil water recharge from precipitation did not occur (Fig. 4*D*); thus, the increased ET in spring further contributed to drought-related soil water limitations (primarily from reduced precipitation) during summer. Evaporative cooling (from LE) inhibits H flux from ecosystems to the atmosphere and prevents extreme heating on the surface and in the lower atmosphere during the period of peak insolation in summer (baseline shown in Fig. 4*A*). The reduction in ET due to water limitations during summer 2012 weakened this cooling effect, shifting the partitioning of available energy toward H, and thus contributed to a positive (enhancing) ecosystem heating feedback (Fig. 4*B*). Consequently, the positive effect of higher carbon uptake during the warmer spring comes at the cost of soils drying out earlier, and thus potentially exacerbating drought and increasing summer heating in regions with limited soil moisture reserves.

Drier soils cause feedback mechanisms that amplify the coupling between drought and heat when ET is inhibited (26). Previous evidence for such heating feedback amplification from spring soil-moisture deficits was shown for European summer heat waves and also indicated that early summer precipitation can mitigate the effect (13). The central Great Plains, which includes parts of the Midwest, is a region with strong biosphere-atmosphere coupling during summer (i.e., soil moisture also has substantial impacts on local precipitation) (27). Soil moisture deficits thus have a positive (enhancing) feedback on drought conditions in this region, highlighting the implications of potential water depletion from earlier vegetation activity during warm spring. Although our analyses cannot quantify the actual heating contribution from the ecosystem feedback during the 2012 summer drought, these results provide further evidence for a linkage between earlier vegetation activity during a warmer spring, the associated depletion of soil water, and the enhanced heating from reductions in evaporative cooling (28) during subsequent summer drought (29). The combination of warm spring and summer drought can also affect species composition based on plant ecophysiology (*SI Appendix*).

Although exceptional for the past century, it was found that the sequence of atmospheric circulation patterns that caused the 2012 drought resulted mostly from natural variability in climate (17). However, large-scale droughts, such as the 2012 drought, are projected to become more prevalent with global warming (18, 20). Climate projections from the Coupled Model Intercomparison

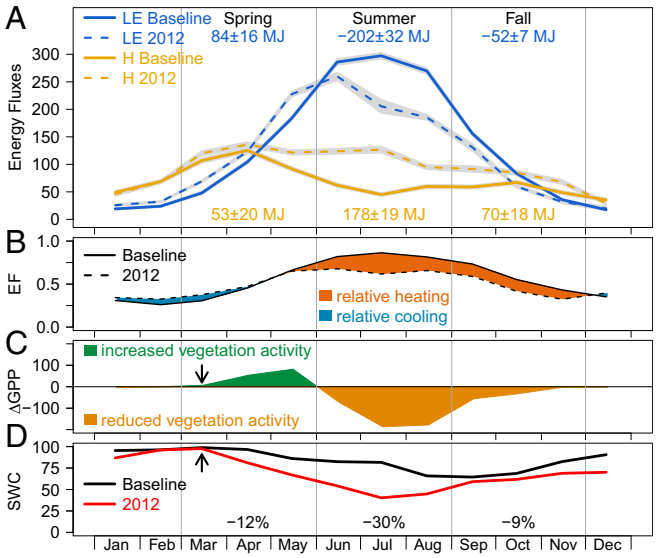

Fig. 4. Earlier vegetation activity contributed to changes in water and energy fluxes during summer. (*A*) Ensemble mean of monthly LE flux and H flux (both in MJ m^{-2} mo^{-1}) for 2012 and the baseline of 2008–2010 from flux tower measurements in the Midwest (n = 3, sites US-KON, US-KFS, and US-MMS). Numbers a top represent the mean seasonal anomalies and their uncertainties from Monte-Carlo simulations (also gray shading). (*B*) EF for 2012 and baseline with shading indicating integrated anomalies. (*C*) Anomalies of GPP (g C m^{-2} mo^{-1}) show earlier vegetation activity inferred by photosynthetic activity in 2012 relative to baseline. Arrows indicate the earlier start of vegetation activity (GPP) and an earlier drawdown in (*D*) volumetric soil water content (SWC, percentage of saturation), and numbers denote mean seasonal anomalies. Further details on net carbon fluxes, precipitation deficits, and vegetation activity can be found in *SI Appendix*, Figs. S10 and S11.

Project Phase 5 (CMIP5) show warmer spring and drier summer mean conditions by the end of this century across the CONUS (*SI Appendix*, Fig. S1), implying that such years will likely occur more frequently. Whether the response observed in 2012 is representative of what can be expected under future climate change remains subject to large uncertainty. For instance, CO_2-induced increases in plant water-use efficiency are expected to affect plant function strongly, and could influence the effects of drought (30). Because the uncertainties in climate projections are linked to uncertainties in carbon cycle feedbacks (31), it is important to better understand the response of the biosphere to seasonal climate anomalies and their effects on the annual carbon balance. Although the impact of a concurrent warmer spring and summer drought depends on the specific climate anomalies (*SI Appendix*), the 2012 event serves as an example that enables the quantification of the impact of such climate anomalies on the carbon and water cycles, and the surface energy budget.

Conclusions

We conclude that the warm spring reduced the impact of the 2012 summer drought on net annual carbon uptake across the United States. Regional differences played a major role for the continental-scale carbon balance in 2012: increased spring uptake in the Eastern Temperate Forests largely compensated for reduced summer uptake in the Great Plains, emphasizing, in part, the ecosystem service value of these forests. However, the positive carbon cycle effect of a warmer spring and earlier vegetation activity also had potentially detrimental side effects on the water cycle by increasing ET. Consistent with previous evidence on the water cycle effects of spring warming (11), our results suggest that the earlier depletion of soil water can increase ecosystem vulnerability to drought and exacerbate warmer land surface temperatures through reduced evaporative cooling (28) during summer. Further research is needed to understand such vegetation–climate feedbacks better, because they can have large implications for the management of water resources and can potentially further increase the risk of water shortages during the period of highest demand in midsummer (8). Both the magnitude of the spring compensation effect for the carbon cycle and hydrological feedbacks of earlier vegetation activity highlight the importance of accurately predicting ecosystem responses to spring warming.

Materials and Methods

We analyzed the impact of concurrent warmer spring and summer drought on land-atmosphere carbon and water exchange across the United States in 2012 using (*i*) direct measurements of EC, (*ii*) satellite remote-sensing observations from MODIS, and (*iii*) estimates from the atmospheric inverse model CarbonTracker.

Baseline Selection. Anomalies of 2012 were derived relative to the baseline of 2008–2010 (as anomaly = 2012 − baseline) for a consistent reference period across all data streams. The selection of this baseline was constrained by two factors: climate and the availability of in situ measured EC data. The three consecutive years 2008–2010 were closest to the long-term mean of dry and wet areas across the CONUS (*SI Appendix*, Fig. S14). Mean summer precipitation during the baseline was marginally above average (+3%) and showed similar variability compared with the long-term reference period 1982–2011 (*SI Appendix*, Fig. S13 and Tables S5 and S9). The standardized precipitation index (SPI) showed minor deviations from the long-term mean and indicated slightly wetter conditions during the baseline (*SI Appendix*, Fig. S4 and Table S5). We excluded 2011 from the baseline to avoid confounding effects from severe drought in the South and Southwest (25) during that year. Besides these climatological constraints, the number of available EC sites was increasingly limited before 2008.

In Situ EC Data. Direct measurements of half-hourly ecosystem CO_2, water vapor, and energy fluxes were used from 22 sites with at least 5 y of data, representing the major ecosystems across the United States (*SI Appendix*). Croplands were excluded from our analyses of individual sites due to the effect of management on the seasonal timing of ecosystem fluxes, both from crop rotation and from the varying timing of planting/harvest. Individual site data were standardized and rigorously quality-filtered according to established standards within AmeriFlux (32). As suggested by previous comparisons using large EC datasets (33), we used a consistent approach to gap-fill ecosystem fluxes across all sites to quantify total fluxes from a daily to annual scale. Estimates of GPP (photosynthesis) were derived from measured NEP by using nighttime data consisting of respiratory fluxes only (i.e., no photosynthesis) and extrapolating to daytime using temperature response functions fit to moving bins within each year. Positive NEP denotes uptake by the biosphere, and negative values indicate carbon losses. Friction-velocity (u_*) thresholds were specified by the site principal investigators for each site. More details on the flux partitioning and gap-filling methods used are provided by Barr et al. (34). Seasonal impact analysis was limited to sites that experienced drought conditions with precipitation deficits of at least 10% during summer (13 of 22 sites; *SI Appendix*, Table S4). Ensembles were calculated as the daily, monthly, and seasonal mean of integrated fluxes across sites. The level of seasonal compensation (Comp, %) was calculated from the 2012 seasonal anomalies of spring relative to summer carbon uptake as Comp = 100 * (ΔSpring/ΔSummer).

Uncertainty Analyses. The total flux uncertainty includes the components of uncertainties resulting from random measurement errors, gap-filling, and flux partitioning. Flux uncertainty was estimated at the native temporal resolution (half-hourly or hourly) and propagated to aggregate time scales using a Monte-Carlo approach (34, 35). The uncertainties for the 2012 flux anomalies were derived from the uncertainties of the baseline and 2012 as

$$Unc_{Anomaly} = \sqrt{Unc^2_{Baseline} + Unc^2_{2012}}.$$

Satellite Remote-Sensing and Atmospheric Inverse Modeling. Regional and continental scale spatial analyses were based on satellite observations by the National Aeronautics and Space Administration (NASA) MODIS and estimates from the atmospheric inverse model CarbonTracker (CTE2014 and CTE2015) (36). For regional analyses, we used the level I ecoregions (23) provided by the US Environmental Protection Agency (https://www.epa.gov/eco-research/ecoregion-resources). MODIS GPP, ET, and potential ET (PET) data were provided by the Numerical Terradynamic Simulation Group at the University of Montana

(Q. Mu and M. Zhao, ftp://ftp.ntsg.umt.edu/pub/MODIS/NTSG_Products). MODIS EVI data were provided by the US Geological Survey (e4ftl01.cr.usgs.gov/MOLT/MOD13C2.005). CarbonTracker data were provided by Wageningen University (www.carbontracker.eu), and biospheric net fluxes were extracted without fire emissions. Posterior biospheric fluxes in CarbonTracker are derived by optimization of modeled prior net carbon exchange from the Simple-Biosphere-Model-Carnegie-Ames Stanford Approach (SiBCASA) biogeochemical model (37) using atmospheric in situ CO_2 observations (38) and the atmospheric transport model TM5 (*SI Appendix*).

Drought Indices Data. Large-scale precipitation was derived from reanalysis data by NASA's Modern-Era Retrospective Analysis for Research and Applications (MERRA). Large-scale SPI data were extracted from the Global Integrated Drought Monitoring and Prediction System (GIDMaPS, drought.eng.uci.edu). We also evaluated site-scale SPI based on long-term precipitation records from nearby meteorological stations (*SI Appendix*), but only used these data to quantify drought across ensembles of multiple sites (*SI Appendix*, Fig. S4). Furthermore, we used the Evaporative Stress Index (ESI), which is a physically based drought index linked to evaporative demand that includes both land-surface (via ET) and atmospheric feedbacks (via PET) (39). The ESI was calculated from observed ET and PET (estimated by Penman–Monteith parameterization) as ESI = 1 − (ET/PET). Evaporative fraction (EF) was calculated from EC-measured LE and H fluxes as EF = LE/(LE+H), with values larger than 0.5 indicating that LE (ET in energy units) is dominating the available energy transfer to the atmosphere.

Analyses. Seasons were classified according to the meteorological definition, with spring as the 3-mo period of March–May and summer as the 3-mo period of June–August. The software R was used for all statistical data analyses (R Development Core Team, www.r-project.org).

ACKNOWLEDGMENTS. We acknowledge support from the Carbon Dioxide Information Analysis Center at the Oak Ridge National Laboratory, particularly B. Yang. We thank D. M. Ricciuto for assistance with the gap-filling of climate data and M. Sikka for remote-sensing data processing. We thank all data contributors for this synthesis study, particularly P. Blanken, G. Bohrer, D. Bowling, S. Burns, K. L. Clark, D. Hollinger, S. Ma, Q. Mu, K. A. Novick, S. A. Papuga, F. Rahman, and M. Zhao. We thank K. A. Novick, G. Bohrer, E. van Gorsel, and E. Paul-Limoges for helpful comments on the manuscript. We also appreciate the constructive comments of the reviewers and the editor. This research was supported by the European Commission's FP7 Marie Curie International Outgoing Fellowship Grant 300083 (to S.W.). Funding for the AmeriFlux Management Project was provided by the US Department of Energy's Office of Science (Contract DE-AC02-05CH11231). T.F.K. acknowledges support from a Macquarie University Research Fellowship. J.B.F. carried out the research at the Jet Propulsion Laboratory, California Institute of Technology, under a contract with the National Aeronautics and Space Administration, and acknowledges support from NASA's Terrestrial Hydrology Program. A.D.R. acknowledges support from the National Science Foundation (NSF), through the Macrosystems Biology program (Award EF-1065029) and the LTER program (DEB-1114804). M.E.L. acknowledges support from NASA ROSES (Award 0486V-874F). N.A.B. acknowledges support from the NSF EPSCoR program (EPS-0553722 and EPS-0919443) and the LTER program at the Konza Prairie Biological Station (DEB-0823341). W.P. and I.T.v.d.L.-L. acknowledge funding from NWO (SH-060-13) for computing time. I.T.v.d.L.-L. received financial support from OCW/NWO for ICOS-NL.

1. Dai A (2013) Increasing drought under global warming in observations and models. *Nat Clim Chang* 3(1):52–58.
2. Trenberth KE, et al. (2014) Global warming and changes in drought. *Nat Clim Chang* 4(1):17–22.
3. IPCC (2013) *Climate Change 2013: The Physical Science Basis. Contribution of Working Group I to the Fifth Assessment Report of the Intergovernmental Panel on Climate Change*, eds Stocker TF, et al. (Cambridge Univ Press, Cambridge, UK).
4. Ciais P, et al. (2005) Europe-wide reduction in primary productivity caused by the heat and drought in 2003. *Nature* 437(7058):529–533.
5. Keenan TF, et al. (2014) Net carbon uptake has increased through warming-induced changes in temperate forest phenology. *Nat Clim Chang* 4(7):598–604.
6. Wolf S, et al. (2013) Contrasting response of grassland versus forest carbon and water fluxes to spring drought in Switzerland. *Environ Res Lett* 8(3):035007.
7. Angert A, et al. (2005) Drier summers cancel out the CO_2 uptake enhancement induced by warmer springs. *Proc Natl Acad Sci USA* 102(31):10823–10827.
8. Melillo JM, Richmond TC, Yohe GW (2014) *Climate Change Impacts in the United States: The Third National Climate Assessment* (US Global Change Research Program, Washington, DC).
9. Seneviratne SI, et al. (2012) Changes in climate extremes and their impacts on the natural physical environment. *Managing the Risks of Extreme Events and Disasters to Advance Climate Change Adaptation. A Special Report of Working Groups I and II of the Intergovernmental Panel on Climate Change (IPCC)*, eds Field CB, et al. (Cambridge Univ Press, Cambridge, UK), pp 109–230.
10. Yi C, Pendall E, Cias P (2015) Focus on extreme events and the carbon cycle. *Environ Res Lett* 10(7):070201.
11. Parida BR, Buermann W (2014) Increasing summer drying in North American ecosystems in response to longer nonfrozen periods. *Geophys Res Lett* 41(15):5476–5483.
12. Fischer EM, Seneviratne SI, Vidale PL, Lüthi D, Schär C (2007) Soil moisture–atmosphere interactions during the 2003 European summer heat wave. *J Clim* 20(20):5081–5099.
13. Quesada B, Vautard R, Yiou P, Hirschi M, Seneviratne SI (2012) Asymmetric European summer heat predictability from wet and dry southern winters and springs. *Nat Clim Chang* 2(10):736–741.
14. Sheffield J, Wood EF, Roderick ML (2012) Little change in global drought over the past 60 years. *Nature* 491(7424):435–438.
15. Baldocchi D (1997) Measuring and modelling carbon dioxide and water vapour exchange over a temperate broad-leaved forest during the 1995 summer drought. *Plant Cell Environ* 20(9):1108–1122.
16. Teuling AJ, et al. (2010) Contrasting response of European forest and grassland energy exchange to heatwaves. *Nat Geosci* 3(10):722–727.
17. Hoerling M, et al. (2014) Causes and predictability of the 2012 Great Plains Drought. *Bull Am Meteorol Soc* 95(2):269–282.
18. Cook BI, Seager R, Smerdon JE (2014) The worst North American drought year of the last millennium: 1934. *Geophys Res Lett* 41(20):7298–7305.
19. Blunden J, Arndt DS (2013) State of the climate in 2012. *Bull Am Meteorol Soc* 94(8):S1–S258.
20. Overpeck JT (2013) Climate science: The challenge of hot drought. *Nature* 503(7476):350–351.
21. Canadell JG, et al. (2000) Carbon metabolism of the terrestrial biosphere: A multitechnique approach for improved understanding. *Ecosystems (N Y)* 3(2):115–130.
22. Schwalm CR, et al. (2012) Reduction in carbon uptake during turn of the century drought in western North America. *Nat Geosci* 5(8):551–556.
23. Omernik JM (1987) Ecoregions of the conterminous United States. *Ann Assoc Am Geogr* 77(1):118–125.
24. Friedl MA, et al. (2014) A tale of two springs: Using recent climate anomalies to characterize the sensitivity of temperate forest phenology to climate change. *Environ Res Lett* 9(5):054006.
25. Parazoo NC, et al. (2015) Influence of ENSO and the NAO on terrestrial carbon uptake in the Texas-northern Mexico region. *Global Biogeochem Cycles* 29(8):1247–1265.
26. Seneviratne SI, et al. (2010) Investigating soil moisture-climate interactions in a changing climate: A review. *Earth Sci Rev* 99(3-4):125–161.
27. Koster RD, et al.; GLACE Team (2004) Regions of strong coupling between soil moisture and precipitation. *Science* 305(5687):1138–1140.
28. Yin D, Roderick ML, Leech G, Sun F, Huang Y (2014) The contribution of reduction in evaporative cooling to higher surface air temperatures during drought. *Geophys Res Lett* 41(22):7891–7897.
29. Richardson AD, et al. (2013) Climate change, phenology, and phenological control of vegetation feedbacks to the climate system. *Agric For Meteorol* 169:156–173.
30. Keenan TF, et al. (2013) Increase in forest water-use efficiency as atmospheric carbon dioxide concentrations rise. *Nature* 499(7458):324–327.
31. Friedlingstein P, et al. (2014) Uncertainties in CMIP5 Climate Projections due to Carbon Cycle Feedbacks. *J Clim* 27(2):511–526.
32. Boden TA, Krassovski M, Yang B (2013) The AmeriFlux data activity and data system: an evolving collection of data management techniques, tools, products and services. *Geoscience Instrumentation, Methods, and Data Systems* 2(1):165–176.
33. Desai AR, et al. (2008) Cross-site evaluation of eddy covariance GPP and RE decomposition techniques. *Agric For Meteorol* 148(6-7):821–838.
34. Barr AG, et al. (2013) Use of change-point detection for friction–velocity threshold evaluation in eddy-covariance studies. *Agric For Meteorol* 171–172:31–45.
35. Richardson AD, et al. (2012) Uncertainty quantification. *Eddy Covariance. A Practical Guide to Measurement and Data Analysis*, eds Aubinet M, Vesala T, Papale D (Springer, New York), pp 173–209.
36. Peters W, et al. (2010) Seven years of recent European net terrestrial carbon dioxide exchange constrained by atmospheric observations. *Glob Change Biol* 16(4):1317–1337.
37. van der Velde IR, et al. (2014) Terrestrial cycling of $^{13}CO_2$ by photosynthesis, respiration, and biomass burning in SiBCASA. *Biogeosciences* 11(23):6553–6571.
38. Cooperative Global Atmospheric Data Integration Project (2013) Multi-laboratory compilation of atmospheric carbon dioxide data for the period 2000-2012 (obspack_co2_1_PROTOTYPE_v1.0.4b_2014-02-13) (NOAA Global Monitoring Division, Boulder, CO). Available at data.datacite.org/10.3334/OBSPACK/1001. Accessed June 1, 2015.
39. Anderson MC, Norman JM, Mecikalski JR, Otkin JA, Kustas WP (2007) A climatological study of evapotranspiration and moisture stress across the continental United States based on thermal remote sensing: 1. Model formulation. *J Geophys Res Atmos* 112(D10):D10117.